Photoabsorption in carbon monoxide: Stieltjes–Tchebycheff calculations in the separated-channel static-exchange approximation[a)]

N. Padial and G. Csanak

Instituto de Fisica, Universidade Estadual de Campinas, Campinas, Brazil

B. V. McKoy

Arthur Amos Noyes Laboratory of Chemical Physics, California Institute of Technology, Pasadena, California 91125

P. W. Langhoff

Department of Chemistry, Indiana University, Bloomington, Indiana 47401
(Received 13 March 1978)

Theoretical investigations of total and partial-channel photoabsorption cross sections in carbon monoxide are reported employing the Stieltjes–Tchebycheff (S–T) technique and separated-channel static-exchange calculations. Pseudospectra of discrete transition frequencies and oscillator strengths appropriate for individual excitations of each of the six occupied molecular orbitals are constructed using Hartree–Fock core functions and normalizable Gaussian orbitals to describe the photoexcited and ejected electrons. Use of relatively large basis sets of compact and diffuse functions insures the presence of appropriate discrete Rydberg states in the calculations and provides sufficiently dense pseudospectra for the determination of convergent photoionization cross sections from the S–T technique. The calculated discrete vertical electronic excitation spectra are in very good agreement with measured band positions and intensities, and the partial-channel photoionization cross sections are in correspondingly good accord with recent electron–electron (e,2e) coincidence, synchrotron-radiation, and line-source branching-ratio measurements. Predicted resonance features in the X, B, $O2s^{-1}$, and carbon K-shell channels are in particularly good agreement with the positions and intensities in the measured cross sections. A modest discrepancy between experiment and theory in the A-channel cross section is tentatively attributed to channel-coupling mechanisms associated with opening of the 1π shell. The total vertical electronic S–T photoionization cross section for parent-ion production is in excellent agreement with recent electron–ion coincidence measurements. Comparisons are made between ionization processes in carbon monoxide and in the previously studied nitrogen molecule, and similarities and differences in the respective cross sections are clarified in terms of conventional molecular-orbital theory.

I. INTRODUCTION

Experimental and theoretical photoabsorption studies have long provided complementary information useful for disentangling the various discrete excited states in diatomic molecules and for clarifying the intensities of the corresponding transitions.[1,2] By contrast, the intensities of molecular photoionization processes have proved somewhat more difficult to separate experimentally, since one or more of the electrons is in a continuum state in this case and a number of competing channels generally contribute to the total cross section at a given frequency. Consequently, total absorption measurements cannot provide unambiguous spectra-information in the photoionization continuum. Moreover, reliable *ab initio* theoretical studies of photoionization cross sections in diatomics are generally unavailable, in spite of the development of a number of computational approaches for constructing the required continuum molecular wavefunctions.[3–8] Recent refinements in experimental techniques and in theoretical approaches, however, now provide the basis for quantitative studies of photoionization processes in diatomic molecules.[9] In particular, photoionization branching-ratio measurements, obtained from synchrotron-radiation,[10] line-source,[11,12] and electron–electron ($e,2e$) coincidence[13] studies, and corresponding electron–ion coincidence measurements of parent-ion and dissociative cross sections,[14,15] provide additional information for disentangling and assigning the various continuum electronic excitations. Such detailed experimental studies reveal the presence of prominent resonance features in specific channels which are not clearly distinguishable in total photoabsorption cross section measurements.[16,17] Corresponding refinements in theoretical techniques[18–23] have also proved useful for predicting total cross sections[18,19] and for interpreting and clarifying the electronic excitations responsible for structures in the measured partial-channel photoabsorption cross sections.[20–23]

In the present paper, detailed theoretical studies of total and partial-channel vertical electronic photoabsorption cross sections in carbon monoxide are reported, complementing previously described studies in the case of molecular nitrogen.[22,23] The Stieltjes–Tchebycheff (S–T) technique is employed,[24,25] in conjunction with calculations of discrete pseudospectra in the separated-channel static-exchange approximation,[22,23] in constructing the relevant vertical electronic cross sections. As in the case of molecular nitrogen, the present

[a)]Supported in part by the US–Latin American Cooperative Science Program, NSF(OIP)-CNPq (Brazil), and by the Donors of the Petroleum Research Fund, administered by the American Chemical Society.

 0021-9606/78/6907-2992$01.00

results are in very good agreement with the measured positions and strengths of discrete transitions,[26–29] with the measured partial-channel photoionization cross sections for the production of the electronic molecular-ion states considered,[10–13] and with the total photoionization cross section for parent-ion production.[14,15] Predicted shape resonances in the $(5\sigma^{-1})X^2\Sigma^+$, $(4\sigma^{-1})B^2\Sigma^+$, and $(3\sigma^{-1})^2\Sigma^+$ valence photoionization channels, and in the carbon $(2\sigma^{-1})$ K-edge cross section, are found to be in excellent accord with the photoabsorption[10,11] and electron-scattering measurements.[13–15] The calculated $(1\pi^{-1})A\,^2\Pi$ cross section is in general agreement with the measured values but falls somewhat below these at higher photon energies, an effect tentatively attributed to channel coupling associated with the opening of the 1π orbital shell. In accordance with the available experimental information,[30] the calculated oxygen $(1\sigma^{-1})$ K-edge cross section also contains high-energy resonance structures. The origins of the resonance features in the various channel cross sections are discussed qualitatively in terms of molecular orbital theory, and similarities and differences between the present results and the previously reported molecular nitrogen cross sections are indicated.[22,23]

The separated-channel static-exchange approximation is described briefly in Sec. II, a qualitative description of the S–T technique is provided for completeness in Sec. III, and the calculated vertical electronic photoabsorption cross sections in carbon monoxide are reported in Sec. IV. Concluding remarks are made in Sec. V.

II. SEPARATED-CHANNEL STATIC-EXCHANGE APPROXIMATION

The vertical electronic photoabsorption cross section of a diatomic molecule, calculated in a body-fixed coordinate system, can be written as a sum of partial cross sections for the energetically open channels in the form[31]

$$\sigma(\omega) = \sum_{\Gamma} \sigma_{\Gamma}(\omega)\,. \tag{1}$$

Here, the partial-channel cross sections are (Hartree atomic units are employed unless otherwise indicated)

$$\sigma_{\Gamma}(\omega) = (2\pi^2/c) g_{\Gamma}(\omega)\,, \tag{2}$$

and

$$g_{\Gamma}(\omega) = (2/3)\omega \left| \langle \Psi_{\Gamma}^{-} | \mu | \Psi_0 \rangle \right|^2 \tag{3}$$

is the oscillator-strength density for the channel Γ.[32] In Eq. (3), Ψ_{Γ}^{-} represents any of the unity-normalized bound states of the molecule ($\omega = \epsilon_i - \epsilon_0$), or refers to a molecular continuum function ($\omega = \epsilon - \epsilon_0$) satisfying incoming boundary conditions appropriate for electrons incident upon the ionic state associated with the channel Γ.[33,34] The functions Ψ_{Γ}^{-} are generally well approximated as combinations of various valence and Rydberg configurations in the discrete region of the spectrum. In the continuum they contain scattered-wave components that give the inelastic amplitudes for all other open channels and, in particular, they include the various autoionizing states associated with Rydberg series above the first ionization threshold. Moreover, for molecular systems the electronic functions Ψ_{Γ}^{-}, defined in a body-fixed coordinate system, generally do not correspond to a single partial wave of definite angular momentum, since the potential is anisotropic in this case. Consequently, the Ψ_{Γ}^{-} satisfy differential equations associated with energetically coupled channels which also involve angular-momentum coupling in the body-fixed frame.[35]

In the present development, the problem of energetic channel coupling is overcome by employing a one-electron approximation which identifies the physically distinct electronic excitation mechanisms expected to dominate the photoabsorption cross section of the target system.[20–23] In this way one-electron excitation series are identified for which static-exchange potentials can be constructed employing Hartree–Fock wavefunctions for the core states. Consequently, the present development neglects the effects of energetic channel coupling and of core relaxation upon photoexcitation. Some allowance is made for relaxation effects, however, by employing experimentally determined ionization potentials rather than Koopmans values in the development. As is indicated in more detail in the following section, the angular-momentum coupling problem within each electronic channel is solved completely by employing functions of good molecular symmetry type.

The electronic ground state of carbon monoxide $X^1\Sigma^+$ is described in the Hartree–Fock approximation as[36]

$$(1\sigma^2 2\sigma^2 3\sigma^2 4\sigma^2 1\pi^4 5\sigma^2)^1\Sigma^+. \tag{4}$$

Consequently, there are 13 distinct one-electron dipole series corresponding to individual excitations of the six occupied molecular orbitals.[2] These excitation series are designated in the forms

$$(5\sigma^{-1}k\sigma)\,^1\Sigma^+,\quad (5\sigma^{-1}k\pi)\,^1\Pi\,, \tag{5a}$$

$$(1\pi^{-1}k\sigma)\,^1\Pi,\quad (1\pi^{-1}k\pi)\,^1\Sigma^+,\quad (1\pi^{-1}k\delta)\,^1\Pi\,, \tag{5b}$$

$$(4\sigma^{-1}k\sigma)\,^1\Sigma^+,\quad (4\sigma^{-1},k\pi)\,^1\Pi\,, \tag{5c}$$

$$(3\sigma^{-1}k\sigma)\,^1\Sigma^+,\quad (3\sigma^{-1}k\pi)\,^1\Pi\,, \tag{5d}$$

$$(2\sigma^{-1}k\sigma)\,^1\Sigma^+,\quad (2\sigma^{-1}k\pi)\,^1\Pi\,, \tag{5e}$$

$$(1\sigma^{-1}k\sigma)\,^1\Sigma^+,\quad (1\sigma^{-1}k\pi)\,^1\Pi\,. \tag{5f}$$

In each case a one-electron problem

$$(h_{\Gamma} - \epsilon)\phi_{\Gamma} = 0 \tag{6}$$

is constructed, where

$$h_{\Gamma} = T + V + V_{\Gamma} \tag{7}$$

is the appropriate static-exchange Hamiltonian. In Eq. (7), T and V refer to the kinetic-energy and nuclear-framework potential-energy operators, respectively, and V_{Γ} is the static-exchange potential appropriate for the channel Γ. For excitations out of σ orbitals ($\sigma \to \sigma, \pi$),

$$V_{\Gamma} = \sum_i (2J_i - K_i) + J_{\Gamma} + K_{\Gamma}\,, \tag{7'}$$

where the sum i is over the Coulomb J_i and exchange K_i operators of the unexcited doubly occupied core orbitals, and Γ refers to the σ molecular orbital excitation

under consideration. By contrast, for π orbitals ($\pi \rightarrow \sigma, \pi, \delta$) the appropriate static-exchange potentials assume somewhat more complex forms, a situation that has been discussed previously in some detail.[37] Since the static-exchange Hamiltonian of Eqs. (6) and (7) contains a $V^{(N-1)}$ potential,[38,39] the bound states of Eq. (6) correspond to so-called improved virtual orbitals (IVO).[40] These are expected to provide useful approximations to the appropriate valence[41] and Rydberg[42] states in carbon monoxide. The associated continuum states are expected to provide reliable approximations to the corresponding one-electron photoionization spectra in carbon monoxide, for reasons previously discussed.[43]

Since the Hamiltonian of Eq. (7) is Hermitian, the solutions of Eq. (6) form an orthogonal set. However, the lowest-energy bound states obtained from Eq. (6), corresponding to the occupied orbitals of the appropriate symmetry, generally differ from those of Eq. (4), since the latter are obtained from a different Hartree–Fock Hamiltonian than that of Eqs. (7). Although the differences in respective orbitals are generally small,[42] it is convenient to deal with a properly orthonormalized spectrum of occupied and virtual orbitals in each case, particularly in connection with evaluation of transition moments. Consequently, as is discussed further in the following section, the excited orbital solutions of Eqs. (6) and (7) obtained here are explicitly orthogonalized to the occupied canonical Fock orbitals in each case. It is anticipated that the photoabsorption cross sections so obtained will not differ significantly from those obtained without the orthogonality constraint, except perhaps at very low excitation energies.[44,45] Those features of the calculated cross sections that are potentially sensitive to the orthogonality constraint are discussed explicitly at appropriate points in the subsequent text.

III. STIELTJES–TCHEBYCHEFF TECHNIQUE

The potentials appearing in Eqs. (6) and (7) are noncentral and nonlocal, necessitating the introduction of special computational procedures. Although such equations can be solved in a variety of ways in the case of molecular hydrogen,[18] which is approximately spherical, convergence difficulties arise for larger more anisotropic molecules.[35] In the present studies, Eqs. (6) and (7) are solved employing the Roothaan–Hartree–Fock procedure,[36] and the Stieltjes–Tchebycheff technique is applied to the resulting discrete pseudospectra.[24,25] In this way, photoexcitation and ionization cross sections are obtained in carbon monoxide in the separated-channel static-exchange approach without further computational approximation, and the difficult explicit construction of molecular-symmetry continuum functions satisfying asymptotic boundary conditions is avoided.

Following the Roothaan–Hartree–Fock procedure, expansions in discrete basis sets of functions that are explicitly orthogonalized to the occupied canonical Fock orbitals are employed to obtain variational solutions of Eq. (6) in the form,

$$\langle \phi_i^\Gamma | h_\Gamma | \phi_j^\Gamma \rangle = \epsilon_i^\Gamma \delta_{ij}, \tag{8a}$$

$$\langle \phi_i^\Gamma | \phi_j^\Gamma \rangle = \delta_{ij}, \quad i,j = 1,2,\ldots,N. \tag{8b}$$

Associated pseudospectra of transition frequencies and oscillator strengths are obtained from the expressions

$$\tilde{\epsilon}_i^\Gamma = \epsilon_\Gamma + \epsilon_i^\Gamma, \tag{9a}$$

$$\tilde{f}_i^\Gamma = (2/3)\tilde{\epsilon}_i^\Gamma |\langle \phi_i^\Gamma | \mu | \phi_\Gamma \rangle|^2, \tag{9b}$$

where the experimental ionization potential is used for ϵ_Γ,[46–48] ϕ_Γ is the occupied orbital of the active electron in the channel Γ, and μ is the dipole moment operator.

The pseudospectrum of Eqs. (9) provides the information required in the construction of the corresponding photoionization continuum following the S–T development.[24,25] It is important to recognize that the S–T technique does not refer to a finite-energy-interval averaging of the primitive pseudospectrum [Eqs. (9)]. Such bin-smoothing approaches generally give unreliable continua, particularly when applied to the somewhat irregular pseudospectra obtained employing nonlocal potentials. Rather, in following the S–T technique, the spectral moments (the channel label Γ is dropped here for clarity)

$$\tilde{S}_N(-k) = \sum_{i=1}^{N} \tilde{f}_i \tilde{\epsilon}_i^{-k}, \quad k = 0,1,\ldots,2n-1, \tag{10}$$

($n \ll N$) are constructed, and employed in calculations of moment-theory spectra[24,25]

$$\{\epsilon_i(n), f_i(n)\}, \quad i = 1,2,\ldots,n, \tag{11}$$

satisfying

$$\tilde{S}_N(-k) = \sum_{i=1}^{n} f_i(n)\epsilon_i(n)^{-k}. \tag{12}$$

When the $\tilde{S}_N(-k)$ furnish accurate approximations to the correct invariant spectral moments $S(-k)$ of the molecular system,[49] the spectrum of Eq. (11) can be employed in a smoothing procedure. Specifically, bounding approximations are constructed to the cumulative oscillator-strength distribution, and these are differentiated in the S–T sense with respect to the energy variable.[25] The oscillator-strength density so obtained exhibits resonancelike structures at the appropriate discrete transition frequencies, and is smooth in the photoionization continuum.[24]

As alternatives to the negative-integer power moments of Eq. (10), other appropriately defined integrals or generalized moments can be employed in conjunction with the S–T technique.[50] Moreover, in computational applications it is generally unnecessary to calculate the moments of Eq. (10) and to solve Eqs. (12). Rather, the recurrence coefficients[51]

$$(\alpha_k, \beta_{k-1}), \quad k = 0,1,\ldots,n-1, \tag{13}$$

for the polynomials orthogonal with respect to the oscillator-strength density are calculated directly from the primitive spectrum of Eq. (9) employing a stable computational algorithm.[24] The corresponding moment-theory spectrum [Eq. (11)] is obtained from the poles and residues of appropriately defined orthogonal-polynomial rational fractions.[51]

The recurrence coefficients of Eq. (13) provide cri-

teria for estimating the convergence of the quantum-mechanical calculations used in constructing the primitive pseudospectrum [Eq. (9)]. Moreover, the calculated coefficients can be supplemented with additional $\alpha_k\beta_k$ values chosen to extrapolate smoothly in k to the asymptotic expressions,

$$\alpha_\infty = 1/(2\epsilon_t), \tag{14a}$$

$$\beta_\infty = 1/(4\epsilon_t)^2, \tag{14b}$$

where ϵ_t is the threshold for photoionization.[24] In this way, a complete set of recurrence coefficients is obtained, and the S–T technique can provide completely convergent oscillator-strength distributions and densities.

IV. PHOTOABSORPTION CROSS SECTIONS IN CARBON MONOXIDE

A Hartree–Fock function of good quality is constructed near the equilibrium internuclear separation (R_e = 2.13 a.u.) in carbon monoxide employing a $(10s, 5p, 1d)/[3s, 2p, 1d]$ contracted Gaussian basis.[52] The resulting occupied orbitals are used to form the static-exchange potentials and individual channel Hamiltonians of Eqs. (7). The basis functions used in constructing the occupied Fock orbitals are supplemented with additional functions in each case, providing up to ~60 compact and diffuse Gaussian functions for solution of Eq. (6). Specifically, in σ symmetry four additional s- and p-type functions are placed on both the C and O centers, and nine s- and p-type functions are placed at the center of mass (c.m.), employing exponents ranging from 2.0 to 0.001. In π symmetry, six additional s- and p-types on both C and O centers, and nine s- and p-types at the c.m., are used, with the same exponent range as in σ symmetry. Finally, in δ symmetry, seven additional d-type functions are placed on the C and O centers, and 10 at the c.m., again employing a 2.0 to 0.001 exponent range. As indicated above, these basis sets for solution of Eq. (6) are explicitly orthogonalized to the occupied Fock orbitals in each case. It is found that the partitioning of oscillator strength between the discrete and continuum regions, and the general nature of the continuum photoionization cross section, is relatively insensitive to basis set provided at least ~15–20 Gaussians are employed. By contrast, the number of discrete states obtained in each case is quite sensitive to the number of very diffuse basis functions employed in the calculations, although the first few discrete states are generally stable to basis-set changes. The results presented in the following section correspond to the use of pseudospectra with $N \cong 40$, 30, and 25 for virtual orbitals of σ, π, and δ symmetry, respectively. These pseudospectra provide good approximations to the first few members of the individual Rydberg series, and are sufficiently dense in the continuum regions to provide convergent S–T photoionization cross sections, as indicated below.

The S–T cross sections obtained from the calculated pseudospectra are found to be smooth and stable at approximately eighth order in each case, and to converge fully when the extension procedure of Sec. III is employed. In view of the large basis sets employed in the present calculations, it is highly unlikely that the introduction of additional functions will result in significant changes in the calculated cross sections. Consequently, it is anticipated that the present results give convergent approximations to the photoabsorption cross sections in carbon monoxide in the separated-channel static-exchange approximation. The S–T results are compared with available measurements in the following subsections.

A. Valence shell partial-channel cross sections

1. $(5\sigma^{-1})X\,^2\Sigma^+$ channel (I.P. = 14.0 eV)

The calculated discrete transition series for $5\sigma \rightarrow n\sigma$ and $n\pi$ excitations in CO are shown in Table I, and are compared there with corresponding measured values. The $5\sigma \rightarrow n\sigma$ transitions are grouped into $(ns\sigma, np\sigma)$ excitation series, with the former evidently considerably weaker than the latter, in accordance with measured band intensities. Both series, and the $n\pi$ series as well, are evidently monotonically decreasing in intensity. Agreement between the calculated and observed $5\sigma \rightarrow n\sigma$ transition energies (corresponding to band maxima when appropriate) shown in Table I is apparently excellent. The strong first member of the $5\sigma \rightarrow n\pi$ series corresponds to a $\sigma \rightarrow \pi^*$ valence transition into the $A(2p\pi)\,^1\Pi$ state. The calculated f number for this transition is in accord with recent intensity measurements ($f \sim 0.2$),[14,28] and the predicted positions and strengths of the IVO $5\sigma \rightarrow n\pi$ Rydberg series are evidently in excellent agreement with the measured spectra.

The earlier IVO excitation-energy calculations using Slater basis functions[42] shown in Table I are evidently in very good agreement with the present results. As indicated in the table, the earlier calculations predict $3d\sigma$ and $3d\pi$ excitations at 12.5 and 12.6 eV, respectively. These do not appear in the present calculations, as a consequence of the lack of diffuse d-type basis functions in σ and π symmetry. Since the intensities of transitions into these orbitals are expected to be relatively weak,[27] the apparent deficiency is not a significant one for the purposes of the present investigation. Similarly, previous experience indicates that d-type function deficiency will have modest effect on the calculated $\sigma \rightarrow k\sigma$ and $k\pi$ photoionization continua.[23] The previously reported RPA transition intensities shown in Table I are in general accord with the present values, except perhaps in the case of the B state. In view of the relatively small basis employed in these previous investigations, the modest discrepancies obtained are not significant. Finally, the previously reported valence-basis calculation of the A-state excitation energy shown in Table I is evidently in good agreement with the present value.[41]

It is of interest to note in connection with Table I that an expected intense $\sigma \rightarrow \sigma^*$ transition is apparently not present in the theoretical or experimental CO spectra. That is, a strong $X\,^1\Sigma^+ \rightarrow (2p\sigma)\,^1\Sigma^+$ transition is expected in this case on basis of elementary considerations,[1] whereas the theoretical and experimental $^1\Sigma^+$ states in CO, with the possible exception of the tentatively as-

TABLE I. 5σ excitation spectra in CO.

Present results[a]	Experimental values[b,c]	Previous calculations[d-f]
Energy (eV)/f number	Energy (eV)/intensity	Energy (eV)/f number
	$(5\sigma)\,^1\Sigma^+ \rightarrow (ns\sigma)\,^1\Sigma^+$	
10.86/0.00448	10.78 $B(3s\sigma)\,^1\Sigma^+$/weak	11.0/0.048
12.56/0.000447	12.58	12.6
13.18/0.0000062	13.19	···
13.47/ ···	13.44	···
13.71/ ···	13.64	···
	$(5\sigma)\,^1\Sigma^+ \rightarrow (np\sigma)\,^1\Sigma^+$	
11.62/0.0495	11.40 $C(3p\sigma)\,^1\Sigma^+$/strong	11.5/0.12
12.80/0.0244	12.79	12.8
13.28/0.0139	13.29	···
13.52/0.00842	13.54	···
13.76/ ···	13.75	···
	$(5\sigma)\,^1\Sigma^+ \rightarrow (np\pi)\,^1\Pi$	
8.402/0.342	8.40 $A(2p\pi)\,^1\Pi/f \sim 0.2$	8.00/0.22
11.58/0.0110	11.52 $E(3p\pi)\,^1\Pi$/strong	11.5
12.81/0.00685	12.81	12.8
13.29/0.00360	13.30	···
13.53/0.00232	13.67	···
13.85/ ···	···	···

[a]IVO vertical excitation spectra obtained from variational solutions of Eq. (6) employing the basis sets described in Sec. IV.

[b]Spectral assignments and transition energies (corresponding to band maxima when appropriate) taken from the compilations of P. H. Krupenie, Natl. Stand. Ref. Data Ser. Natl. Bur. Stand. **5**, (1966); and E. Lindholm, Ark. Fys. **40**, 111 (1969). See also S. G. Tilford and J. D. Simmons, J. Phys. Chem. Ref. Data **1**, 147 (1972); M. Ogawa and S. Ogawa, J. Mol. Spectrosc. **11**, 393 (1972); and J. Mazeau, C. Schermann, and G. Joyez, J. Electron Spectrosc. Relat. Phenom. **7**, 269 (1975).

[c]Approximate intensity assignments made on basis of the photoabsorption measurements of R. E. Huffman, J. C. Larrabee, and Y. Tanaka, J. Chem. Phys. **40**, 2261 (1964); G. R. Cook, P. H. Metzger, and M. Ogawa, Can. J. Phys. **43**, 1706 (1965); and the electron energy-loss measurements of A. Skerbele, V. D. Meyer, and E. N. Lassettre, J. Chem. Phys. **44**, 4069 (1966); E. N. Lassettre and A. Skerbele, J. Chem. Phys. **54**, 1597 (1971); and G. R. Wight, M. J. Van der Wiel, and C. E. Brion, J. Phys. B **9**, 675 (1976). The approximate intensity designations refer to the entire Rydberg series indicated.

[d]Rydberg transition energies taken from the calculations of H. Lefebvre-Brion, C. M. Moser, and R. K. Nesbet, J. Mol. Spectrosc. **13**, 418 (1964).

[e]The valence $A\,^1\Pi$ transition energy is taken from the calculations of S. V. O'Neil and H. F. Schaefer III, J. Chem. Phys. **53**, 3994 (1970), and refers to an internuclear separation of 2.25 a.u. The calculated value at a separation of 2.13 a.u., which is not tabulated by the authors, is presumably in better accord with the present calculations.

[f]Theoretically determined f numbers taken from the RPA calculations of J. Rose, T. Shibuya, and V. McKoy, J. Chem. Phys. **58**, 74 (1973).

signed $E_0\,^1\Sigma^+$ state,[28] are evidently all Rydberg in nature. Indeed, the lowest effective principal quantum numbers for the observed and calculated $X^1\Sigma^+ \rightarrow {}^1\Sigma^+$ excitations are $n^* \sim 2$. By contrast, the expected intense $\sigma \rightarrow \pi^*$ valencelike transition is apparently present in the $X^1\Sigma^+ \rightarrow (np\pi)\,^1\Pi$ excitation series shown in Table I, and has an effective principle quantum number ~1.5. The situation is evidently similar to that in N_2,[23] in which case the expected intense $3\sigma_g \rightarrow 2p\sigma_u$ or $N \rightarrow V_\sigma$ transition appears in the photoionization continuum, rather than in the discrete spectral region.[1,21,53] On this basis, the presence of a shape resonance can be anticipated in the $5\sigma \rightarrow k\sigma$ photoionization channel in CO.[21]

In Fig. 1(a) are shown the calculated vertical electronic oscillator-strength densities for $5\sigma \rightarrow k\sigma$ and $k\pi$ excitations in CO. An expected shape resonance is indeed present in the $5\sigma \rightarrow k\sigma$ channel at ~24 eV excitation energy, similar to that observed in the $3\sigma_g \rightarrow k\sigma_u$ channel in N_2 at ~23 eV.[23] This feature in both cases can be attributed to the presence of compact $k\sigma^*$ valencelike $(2p\sigma)$ orbitals in the photoionization continua, in accordance with the observations of Mulliken,[53] and the CI calculations of O'Neil and Schaefer.[41] In analogy with the $3\sigma_g \rightarrow k\pi_u$ profile in N_2, the $5\sigma \rightarrow k\pi$ cross section shown in Fig. 1(a) is evidently smaller than that of the $5\sigma \rightarrow k\sigma$ channel near resonance, but dominates the total channel cross section at higher excitation energy. In N_2, however, the inversion symmetry requires precise equality of the $3\sigma_g \rightarrow k\sigma_u$ and $3\sigma_g \rightarrow k\pi_u$ channels at threshold, whereas this is not the case in CO.

Since the $X^2\Sigma^+$ ground state potential-energy curve in CO^+ is deep and is situated vertically above that of ground-state CO,[26] the corresponding Franck–Condon region does not extend far above the 0–0 threshold, and an excellent vibration-rotation-averaged approximation

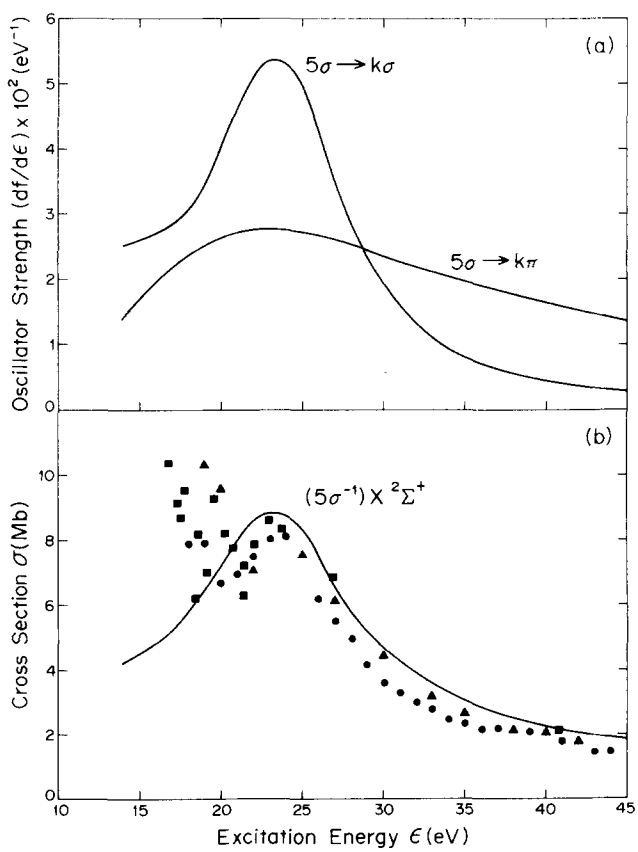

FIG. 1. (a) Vertical electronic IVO S–T oscillator-strength densities for $5\sigma \rightarrow k\sigma$ and $5\sigma \rightarrow k\pi$ ionization in CO. (b) Partial-channel photoionization cross section for the production of $(5\sigma^{-1})X\,^2\Sigma^+$ CO^+ ions; (——), vertical electronic IVO S–T cross section; •, synchrotron-radiation measurements (Ref. 10); ▲, electron–electron $(e, 2e)$ coincidence measurements (Ref. 13); ■, line-source measurements (Ref. 11). 1Mb = 10^{-18} cm^2.

TABLE II. 1π excitation spectra in CO.

Present results[a]	Experimental values[b,c]
Energy (eV)/f number	Energy (eV)/intensity
$(1\pi)\,^1\Sigma^+ \rightarrow (n\pi)\,^1\Sigma^+$	
14.48/0.00237	14.07 $(3p\pi)\,^1\Sigma^+$/weak
15.73/0.00409	15.80
16.20/0.00857	...
16.44/0.0333	...
16.59/0.871	$\sim 14.5\,(\pi \rightarrow \pi^*)\,^1\Sigma^+/f \sim 1.0$[d]
16.79/0.0363	...
$(1\pi)\,^1\Sigma^+ \rightarrow (n\sigma)\,^1\Pi$	
13.33/0.123	13.51G $(3s\sigma)\,^1\Pi/f \sim 0.15$
14.67/0.000080	13.92 $(3p\sigma)\,^1\Pi$/weak
16.05/0.146	15.37
17.03/0.000182	...
$(1\pi)\,^1\Sigma^+ \rightarrow (n\delta)\,^1\Pi$	
15.32/0.0313	15.23 $(3d\delta)\,^1\Pi$/medium[e]
16.02/0.0171	15.98
16.35/0.00966	16.34
16.53/0.00877	16.53

[a]As in Table I.
[b]As in Table I.
[c]As in Table I.
[d]L. Asbrink, C. Fridh, and E. Lindholm, Chem. Phys. **27**, 159 (1978), have recently assigned the $\pi \rightarrow \pi^*$ transition in CO to Lindholm's third unidentified progression (Ref. 27) at ~ 13.7 eV. Previous calculations of S. V. O'Neil and H. F. Schaefer, J. Chem. Phys. **53**, 3994 (1970), give a vertical excitation energy of ~ 15.5 eV for the $(\pi \rightarrow \pi^*)\,^1\Sigma^+$ state. More recent CI studies of $^1\Sigma^+$ states in CO are in good accord with these earlier calculations [S. R. Langhoff (private communication)].
[e]This series is designated by E. Lindholm (footnote b) as $(nd\pi)\,^1\Sigma^+$.

to the partial-channel photoionization cross section for the production of ground state CO^+ is obtained from the sum of the two contributions in Fig. 1(a). In Fig. 1(b) the S–T results for this channel so obtained are compared with recent synchrotron-radiation,[10] line-source,[11] and $(e, 2e)$ electron-coincidence[13] measurements of the partial-channel photoionization cross section. Evidently, all three experimental results are in excellent mutual accord and in good agreement with the calculations above approximately 20 eV excitation energy. It is particularly satisfying that the position and intensity of the shape resonance in this channel are accounted for quantitatively by the present separated-channel static-exchange calculations. A local-potential approximation also predicts a resonance structure in this case, although the result obtained is evidently in poor quantitative agreement with experiment, and is apparently quite sensitive to effective-potential parameter choice.[21]

Below ~ 20 eV excitation energy in CO and N_2 the ionization efficiency is less than unity,[14] and the effects of autoionization, vibrational structure, and fluorescence evidently significantly influence the partial-channel cross sections.[10,11] Consequently, the results of the present calculation, which do not include such effects, cannot be compared in detail with measured values in this region. However, it is appropriate to note that while the present calculations do not provide the correct line shapes in the autoionization region, appropriate averages of measured high-resolution cross sections should compare reasonably well with the S–T results, even in these structured regions, since the total intensities should be adequately predicted in the separated-channel static-exchange approximation. Moreover, when appropriately interpreted, the S–T technique can be employed in atomic and molecular autoionization line shape calculations.[54]

2. $(1\pi^{-1})A\,^2\Pi$ channel (I.P. = 16.9 eV)

In Table II are shown the $1\pi \rightarrow n\sigma$, $n\pi$, and $n\delta$ IVO vertical excitations in CO that fall below the corresponding ionization potential, obtained from Eq. (6) employing the Gaussian basis sets described above. Those states lying above the 14.0 eV 5σ ionization potential are, of course, subject to autoionization into the $X^2\Sigma^+$ channel, in which cases the present calculations can provide zeroth-order wavefunctions for use in appropriate line shape studies. The calculated $1\pi \rightarrow n\pi$ Rydberg series is evidently strongly perturbed by an intense $\pi \rightarrow \pi^*$ transition at ~ 16.6 eV. Note in this connection that the IVO calculations reported here correspond to single-excitation CI employing a frozen or static core,[42] and consequently can accomodate such an interaction, although interactions with the $(ns\sigma)\,^1\Sigma^+$ and $(np\sigma)\,^1\Sigma^+$ states (Table I) are, of course, not included. The position of the $\pi \rightarrow \pi^*$ transition is found to be relatively insensitive to the nature of the basis set employed, whereas the number and type of π Rydberg orbitals obtained, except for the very lowest members of the series, are quite sensitive to the nature of diffuse orbitals employed. The corresponding IVO $\pi \rightarrow \pi^*$ transition in N_2 falls below all the Rydberg $1\pi_u \rightarrow n\pi_g$ states,[23] suggesting that the valence–Rydberg interaction in this approximation is stronger in CO, perhaps as a partial consequence of the lack of inversion symmetry. In addition, the orthogonality constraint employed in the present IVO calculation presumably prevents the valencelike π^* orbital from attaining variationally optimal energy lowering, thereby perhaps exaggerating the interaction with the Rydberg series. The sensitivity of Rydberg–valence interactions is well known, and is treated in previous CI studies in N_2 and related systems.[55,56] These studies show considerable change in the character of valence states and the intensity of valencelike transitions when interactions with underlying Rydberg series are introduced. The estimated experimental band maximum (~ 15 eV) and intensity ($f \sim 1.0$) of the $\pi \rightarrow \pi^*$ transition in CO, however, obtained from electron impact-excitation studies,[14] are in general accord with the present results and previous CI calculations shown in Table II.[41,57] As indicated in the table, an alternative assignment of the $\pi \rightarrow \pi^*$ transition in CO has been made recently at ~ 13.7 eV. In view of the continuing uncertainty of the assignment, detailed studies of the $\pi \rightarrow \pi^*$ transitions in CO and N_2, including vibronic autoionization mechanisms, would seem to be in order. As in the case of N_2, the presence of an intense $\pi \rightarrow \pi^*$ transition in the IVO CO spectrum suggests that the corresponding 1π

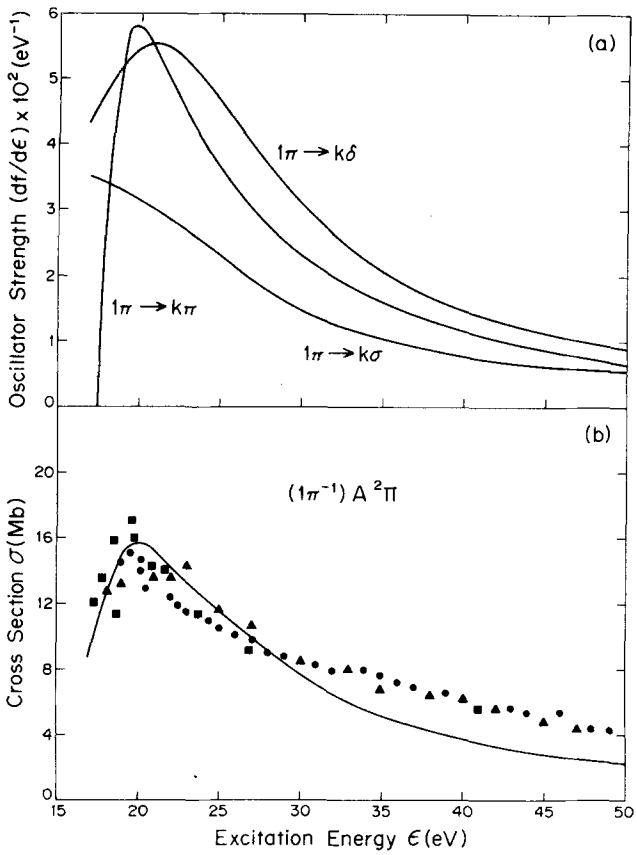

FIG. 2. (a) As in Fig. 1(a) for $1\pi \rightarrow k\sigma$, $1\pi \rightarrow k\pi$, and $1\pi \rightarrow k\delta$ photoionization. (b) As in Fig. 1(b) for production of $(1\pi^{-1})A^2\Pi$ CO^+ ions.

$\rightarrow k\pi$ photoionization continuum will be relatively structureless. Finally, note that the positions and intensities of the first two members of the experimentally identified $(np\pi)\,^1\Sigma^+$ Rydberg series are evidently in general accord with the present IVO calculations, in spite of the very strong perturbation due to the presence of the valence state. Of course, the higher members of the Rydberg series are not adequately described by the present IVO calculations.

The $1\pi \rightarrow n\sigma$ excitations shown in Table II include both $ns\sigma$ and $np\sigma$ series, which evidently differ significantly in relative intensities. The low-lying $1\pi \rightarrow (3s\sigma)\,^1\Pi$ excitation is seen to be in general accord with the measured band maximum and intensity ($f \sim 0.15$).[28] Since this transition falls within the $5\sigma \rightarrow (n\pi)\,^1\Pi$ Rydberg series, interaction between these can be expected. The next member of this $(ns\sigma)$ series evidently falls within the general region of the $\pi \rightarrow \pi^*$ transition. Of course, the $(1\pi \rightarrow ns\sigma)\,^1\Pi$ excitations will interact with the strong $A\,^1\Pi$ resonance in a full CI calculation, and the calculated intensities can be expected to change somewhat when the interaction is included. Nevertheless, since the predicted discrete excitations in this case include strong valencelike $\pi \rightarrow \sigma^*$ transitions, in contrast to the $5\sigma \rightarrow \sigma^*$ spectrum, it can be inferred that the corresponding $1\pi \rightarrow k\sigma$ photoionization continuum will be relatively structureless. The opening of the 1π shell in CO evidently provides an effective potential that can support discrete valencelike σ^* orbitals, in contrast to the situation that obtains in the 5σ case (preceding subsection). In this connection the $1\pi \rightarrow (n\sigma, k\sigma)$ spectrum in CO is generally similar to the previously investigated $1\pi_u \rightarrow (n\sigma_g, k\sigma_g)$ spectrum in N_2.[23]

The $(1\pi \rightarrow n\delta)\,^1\Pi$ series of Table II, which exhibits a conventional intensity variation, is compared with a Rydberg series identified as $(nd\pi)\,^1\Sigma^+$ in this spectral region.[27] The very good agreement with the results of the present IVO calculations would seem to favor the $(nd\delta)\,^1\Pi$ assignment, however.

The three IVO oscillator-strength densities corresponding to vertical $1\pi \rightarrow k\sigma$, $k\pi$, and $k\delta$ ionization in CO are shown in Fig. 2(a). Evidently, the three profiles are quite similar to the analogous $1\pi_u \rightarrow k\sigma_g$, $k\pi_g$, and $k\delta_g$ spectra in N_2.[23] Specifically, the resonancelike structure in the $1\pi \rightarrow k\delta$ profile of Fig. 2(a), involving compact valencelike orbitals in the continuum, has its counterpart in the $1\pi_u \rightarrow k\delta_g$ spectrum in N_2, and the $1\pi \rightarrow k\sigma$ and $k\pi$ profiles are qualitatively similar to the $1\pi_u \rightarrow k\sigma_g$ and $k\pi_g$ spectra in N_2, respectively. However, the $1\pi \rightarrow k\pi$ oscillator-strength density in CO is considerably stronger than its $1\pi_u \rightarrow k\pi_g$ counterpart in N_2. Lack of inversion symmetry in CO apparently allows the transition intensity to appear at higher energy relative to that in N_2, in which case more of the total f number is concentrated in the strong $1\pi_u \rightarrow 1\pi_g$ resonance.[23]

The potential energy curve for the $A\,^2\Pi$ state in CO^+ is deep and shifted only slightly to larger internuclear separation relative to the minimum in the ground $X\,^1\Sigma^+$ state in CO.[26] Consequently, the sum of the three oscillator-strength densities in Fig. 2(a) should provide a good approximation to the vibration–rotation-averaged photoionization cross section for the production of CO^+ in the $A\,^2\Pi$ state. The recent synchrotron-radiation,[10] line-source,[11] and $(e, 2e)$ coincidence[13] measurements of this cross section are compared with the present calculations in Fig. 2(b). Evidently, the three sets of measured values are in good mutual agreement and in general accord with the calculated IVO S–T results, although there is a noticeable discrepancy at higher excitation energy. As in the case of N_2, this discrepancy is presumably a consequence of coupling between the $A\,^2\Pi$ and $B\,^2\Sigma^+$ photoionization channels in CO, related to the opening of the 1π orbital shell, and is investigated in a separate study.

3. $(4\sigma^{-1})\,^2\Sigma^+$ channel (I.P. = 19.7 eV)

The calculated $4\sigma \rightarrow n\sigma$, $n\pi$ IVO excitations lying below the corresponding ionization potential are shown in Table III. The general nature of these series are evidently quite similar to those of the $5\sigma \rightarrow n\sigma$, $n\pi$ series in that both $ns\sigma$ and $np\sigma$ excitations are present, with the former carrying less intensity than the latter, and a strong $\sigma \rightarrow \pi^*$ excitation is present in $^1\Pi$ symmetry. The latter IVO state should be regarded as an additional one since it will mix strongly with the $(1\pi \rightarrow 3s\sigma)\,^1\Pi$ state (Table II) and shift to higher energy upon introduction of CI. Evidently, the $(4\sigma \rightarrow 3s\sigma)\,^1\Sigma^+$ state has not yet been identified in the measured spectra, although the positions and strengths of the higher members of this series are in

TABLE III. 4σ excitation spectra in CO.

Present results[a]	Experimental values[b,c]
Energy (eV)/f number	Energy (eV)/intensity
$(4\sigma)\,^1\Sigma^+ \rightarrow (ns\sigma)\,^1\Sigma^+$	
16.05/0.00657	...
18.04/0.000182	18.20/weak
18.74/0.000123	18.85
19.06/ ...	...
19.28/ ...	...
$(4\sigma)\,^1\Sigma^+ \rightarrow (np\sigma)\,^1\Sigma^+$	
17.42/0.00227	17.08 $(3p\sigma)\,^1\Sigma^+$/medium
18.53/0.00247	18.44
18.97/0.00238	18.95
19.19/0.00220	19.19
19.44/ ...	19.32
$(4\sigma)\,^1\Sigma^+ \rightarrow (n\pi)\,^1\Pi$	
13.75/0.359	13.51 $G(2p\pi)\,^1\Pi/f \sim 0.15$
17.18/0.0372	17.30 $(3p\pi)\,^1\Pi$/medium
18.43/0.00970	18.48
18.93/0.00410	18.97
19.17/0.00229	19.21
19.47/ ...	19.35

[a]As in Table I.
[b]As in Table I.
[c]As in Table I.

general accord with the present IVO calculations. Similarly, the calculated $4\sigma \rightarrow np\sigma$ and $4\sigma \rightarrow n\pi$ series are in good agreement with the two Rydberg series identified in this spectral interval. Of course the intensities in the three 4σ excitation series of Table III, as in the case of the 1π series of Table II, will be rearranged by the effects of autoionization into the underlying continua, which is not explicitly treated here.

The convergent IVO S–T vertical oscillator-strength profiles for $4\sigma \rightarrow k\sigma$ and $k\pi$ transitions are shown in Fig. 3(a). Evidently, the $4\sigma \rightarrow k\sigma$ channel, which does not contain strong discrete transitions (Table III), shows a prominent and broad resonance feature in the continuum peaking at ~32 eV, whereas the $4\sigma \rightarrow k\pi$ continuum profile is broad and flat, with much of the total f number in this channel concentrated in the intense $4\sigma \rightarrow \pi^*$ resonance (Table III). The shape resonance in the $4\sigma \rightarrow k\sigma$ profile is similar to that in the $5\sigma \rightarrow k\sigma$ profile of Fig. 1(a). However, the peak in the $4\sigma \rightarrow k\sigma$ case is shifted somewhat further above the ~24 eV resonance in the $5\sigma \rightarrow k\sigma$ channel than the ~6 eV I.P. difference would suggest. The corresponding $2\sigma_u \rightarrow k\sigma_g$ profile in N_2 shows no prominent resonance structure,[23] since the inversion symmetry disallows transitions into the resonance $k\sigma^*$ continuum orbitals in the case of N_2. The $2\sigma_u \rightarrow k\pi_g$ photoionization profile in N_2, however, is quite similar to the $4\sigma \rightarrow k\pi$ result shown in Fig. 3(a).

As in the case of the $(5\sigma^{-1})X^2\Sigma^+$ state in CO^+, the potential energy curve for the $(4\sigma^{-1})B^2\Sigma^+$ ionic state is deep and situated approximately vertically above the ground state in CO.[26] Consequently, the sum of the two curves in Fig. 3(a) can be compared directly with the measured partial-channel cross section for the production of $B^2\Sigma^+$ state CO^+ ions.[10–13] Figure 3(b) indicates that the three experimental results are in excellent mutual agreement and in good accord with the present calculations. It is particularly satisfying that both the position and intensity of the shape resonance in this channel are correctly accounted for by the present IVO S–T calculations. By contrast, results obtained using local potentials in this case are not quantitatively satisfactory.[21]

B. Valence-shell parent-ion photoionization cross section

A further comparison between the present calculations and experimental values is provided by recent measurement of the total photoionization cross section for parent CO^+ ion production in the 20–50 eV energy region.[14] The theoretical results obtained from the sum of the three contributions of Figs. 1(b), 2(b), and 3(b), each of which corresponds to the production of CO^+ ions, is compared with the recent electron–ion coincidence measurements of this process in Fig. 4.[14] Evidently, the theoretical and experimental results are in very good accord, with only small discrepancies present at low and higher excitation energy. The larger value of the measured cross section in the higher-energy region can presumably be attributed to the small discrepancy present in Fig. 2(b), a consequence of the neglect in the present study of channel coupling, and to contributions from the $C^2\Sigma^+$ state,[26] which is also neglected in the

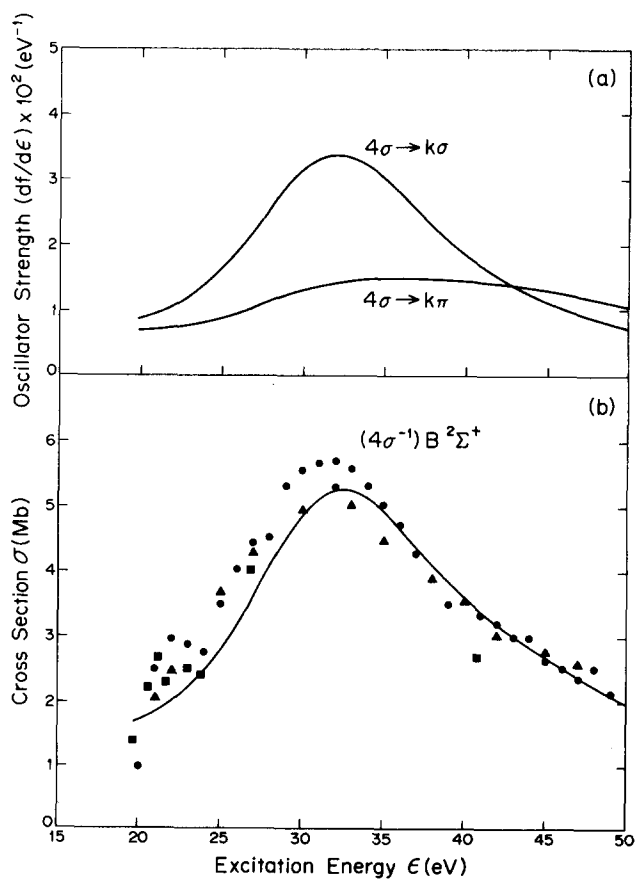

FIG. 3. (a) As in Fig. 1(a) for $4\sigma \rightarrow k\sigma$ and $4\sigma \rightarrow k\pi$ photoionization. (b) As in Fig. 1(b) for production of $(4\sigma^{-1})B^2\Sigma^+$ CO^+ ions.

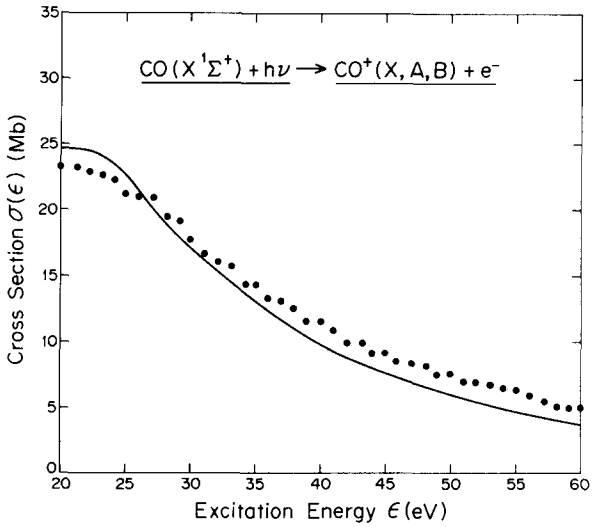

FIG. 4. Total photoionization cross section in CO for the production of parent molecular CO^+ ions; (——), vertical electronic IVO S–T cross section; •, electron–ion coincidence measurements (Ref. 14). 1 Mb = 10^{-18} cm^2.

present study. Although autoionizing structures due to Rydberg states are present in the ~ 20–25 eV interval, the intensity averaging implicit in the electron–ion coincidence measurements evidently provides results in good accord with the IVO calculations, which also correspond to intensity averaging in these highly structured regions. Similarly good agreement to that shown in Fig. 4 between IVO S–T calculations and electron–ion coincidence measurements of the photoionization cross section for parent ion product is obtained in the case of N_2.[23]

C. Dissociative photoionization

Dissociative photoionization in CO resulting in the production of C^+ and O and O^+ and C fragments apparently proceeds primarily through excitation of three molecular ionic states, identified as $C^2\Sigma^+$, $G^2\Sigma^+$, and $(O2s^{-1})^2\Sigma^+$.[13,14] Of these, the first two states correspond to two-electron excitations,[58,59] and are not treated explicitly here. The $(O2s^{-1})^2\Sigma^+$ state corresponds to one-electron 3σ excitation, and consequently is included in the present calculations.

In Fig. 5(a) are shown the vertical IVO S–T $3\sigma - k\sigma$ and $k\pi$ photoionization cross sections in CO. Comparison with Figs. 1(a) and 3(a) indicates the 3σ cross sections are highly similar to those of the 4σ and 5σ orbitals. In particular, the $3\sigma - k\sigma$ contains a shape resonance at ~ 50 eV excitation energy, approximately 12 eV above the 3σ ionization potential (38.3 eV),[46–48] similar to the situation in the 4σ channel.

The two profiles of Fig. 5(a) are added and compared with measured values in Fig. 5(b). Since the $(O2s^{-1})^2\Sigma^+$ ionic state is expected to dissociate completely via crossings with various dissociative states to C^+–O(~ 40%) and C–O^+(~ 60%) fragments,[14] the vibrational degree of freedom can be disregarded in the first approximation, and the sum of the two vertical electronic contributions of Fig. 5(a) can be expected to be in good accord with the results of electron–electron[13] and electron–ion[14] coincidence measurements. Evidently, the agreement shown in Fig. 5(b) between the IVO S–T calculations and the $(O2s^{-1})^2\Sigma^+$ cross section estimate obtained from the electron–ion coincidence measurements is quite satisfactory, whereas the agreement with the $(e, 2e)$ measurements is perhaps only acceptable. Presumably the effects of anisotropy in the angular distribution of photoejected electrons can account for the modest discrepancy in the latter case.

D. Carbon K-shell cross section (I.P. = 296.2 eV)

In Table IV are shown the calculated IVO vertical excitation energies and oscillator strengths for the 2σ molecular orbital, corresponding to the carbon $1s$ atomic orbital, obtained from variational solution of Eqs. (6). Evidently, both $2\sigma \rightarrow ns\sigma$ and $np\sigma$ excitations are present in the calculations, with the intensity of the latter significantly weaker than that of the former. The first two members of the calculated $ns\sigma$ series are in good agreement with the positions and intensities obtained from electron impact-excitation studies,[30] also shown in the table. Although the $3p\sigma$ excitation is apparently not observed in the impact studies,[30] the position assigned on basis of an analogy between core excitations in CO and valence excitations in NO is evident-

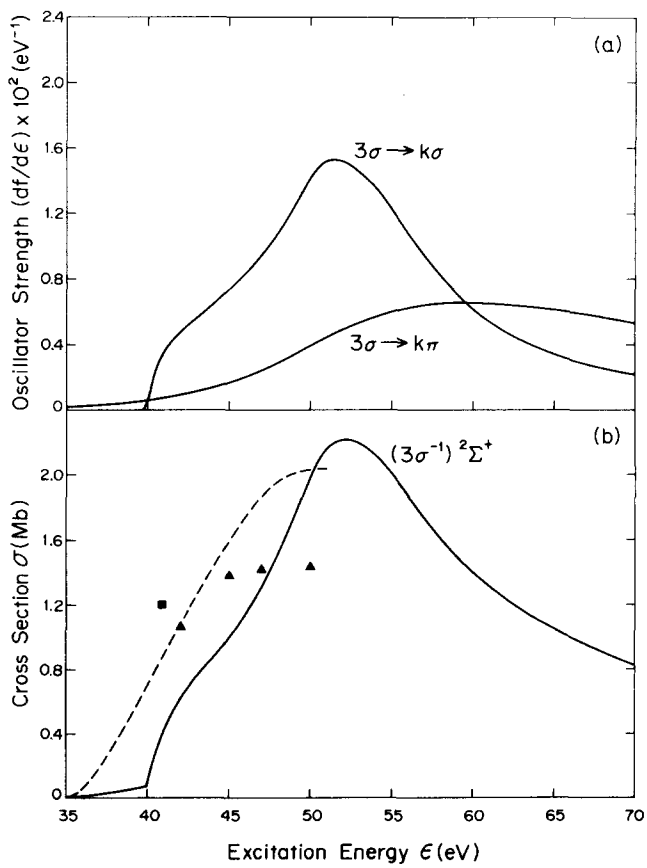

FIG. 5. (a) As in Fig. 1(a) for $3\sigma \rightarrow k\sigma$ and $3\sigma \rightarrow k\pi$ photoionization. (b) As in Fig. 1(b) for production of C^+–O and C–O^+ fragments through the $(3\sigma^{-1})^2\Sigma^+$ state; (-----), estimate obtained from electron–ion coincidence measurements (Ref. 14).

TABLE IV. 2σ (C_K-shell) excitation spectra in CO.

Present results[a]	Experimental values[b]
Energy (eV)/f number	Energy (eV)/intensity
$(2\sigma)^1\Sigma^+ \rightarrow (ns\sigma)^1\Sigma^+$	
291.9/0.0101	292.34($3s\sigma$) $^1\Sigma^+$/medium
294.4/0.00209	294.77
295.2/0.00067	...
295.5/ ...	...
295.7/ ...	...
$(2\sigma)^1\Sigma^+ \rightarrow (np\sigma)^1\Sigma^+$	
293.5/0.000146	294.01($3p\sigma$) $^1\Sigma^+$/not observed[c]
294.8/0.0000072	...
295.3/ ...	...
295.6/ ...	...
295.8/ ...	...
$(2\sigma)^1\Sigma^+ \rightarrow (np\pi)^1\Pi$	
281.3/0.239	287.40($2p\pi$) $^1\Pi$[d]/f = 0.167[e]
293.2/0.00882	293.31/medium
294.8/0.00291	...
295.3/0.00135	...
295.6/0.00074	...

[a]As in Table I.
[b]Values taken from the measurements of G. R. Wight, C. E. Brion, and M. J. Van der Wiel, J. Electron Spectrosc. Relat. Phenom. 1, 457 (1973), except as indicated.
[c]Position assigned on basis of an analogy with the observed NO valence spectrum (see Ref. 61).
[d]M. Tronc, G. C. King, R. C. Bradford, and F. H. Read, J. Phys. B 9, L555 (1977).
[e]R. B. Kay, Ph. E. Van der Leeuw, and M. J. Van der Wiel, J. Phys. B 10, 2513 (1977).

ly in good agreement with the present calculations.[60] Moreover, the predicted very small f number clarifies the experimental failure to observe this state. Finally, the IVO predictions for the strong $2\sigma \rightarrow 2p\pi$ excitation are evidently in semiquantitative accord with the measured position and f number.[15] Evidently, the neglect of core relaxation and related configuration-interaction effects is significant in the case of this valencelike transition. By contrast, the predicted $3p\pi$ excitation, which is more Rydberg-like in character than is the $2p\pi$ excitation, is in good agreement with the measured values.[61]

In Fig. 6(a) are shown the photoionization profiles corresponding to $2\sigma \rightarrow k\sigma$ and $k\pi$ excitations. These are evidently qualitatively similar to the $4\sigma \rightarrow k\sigma$ and $k\pi$ profiles shown in Fig. 3(a), and somewhat similar to those of the 5σ and 3σ excitation spectra, as well, shown in Figs. 1(a) and 5(a), respectively. Moreover, the $2\sigma \rightarrow k\sigma$ channel contribution is similar to the previously reported $1\sigma_g \rightarrow 1\sigma_u$ profile in N_2 in that a high-energy shape resonance is evident at ~ 305 eV excitation energy.[22] As in the previously described $\sigma \rightarrow k\sigma$ channels, the shape resonance in this case can be attributed to the presence of valencelike σ^* molecular orbitals in the photoionization continuum. The $2\sigma \rightarrow k\pi$ profile shown in Fig. 6(a) is small and is a slowly varying function of excitation energy, with much of the total f-sum rule in this channel concentrated in the intense $2p\pi$ excitation. The general shape in this case is similar to the previously reported $1\sigma_u \rightarrow k\pi_g$ channel in N_2.[22]

The two contributions to 2σ photoionization shown in Fig. 6(a) are added and compared with recent electron–ion coincidence measurements of the carbon K-edge cross section in Fig. 6(b). Note that the $2\sigma \rightarrow 2p\pi$ resonance contribution is deleted in the total cross section, since the Stieltjes convention exaggerates its width.[24] Evidently, the experimental and theoretical results are in good accord, except for the presence of a secondary peak in the former, attributable to two-electron excitation,[30,62] which is absent in the latter. These features, and the dynamical effects responsible for subsequent decay of the $(2\sigma^{-1})^2\Sigma^+$ ionic state,[15] are the subject of a subsequent separate investigation.

E. Oxygen K-shell cross section (I.P. = 542.6 eV)

In Table V are shown the calculated 1σ IVO vertical absorption spectra, corresponding to excitation of the oxygen $1s$ orbital, in comparison with available measured values. As in the 2σ case, both $1\sigma \rightarrow ns\sigma$ and $np\sigma$ series are present in the calculations. Although the first members of these calculated series are in good agreement with the measured positions and intensities, the irregualr behavior of the IVO f numbers in these cases suggests that the two series are not fully separated in the calculations. The strong $1\sigma \rightarrow 2p\pi$ resonance in the IVO approximation is in general accord with the measured position, although the effects of relaxation are clearly discernable. Evidently, the next member of the $1\sigma \rightarrow np\pi$ IVO series is in very good agreement with the measured value.

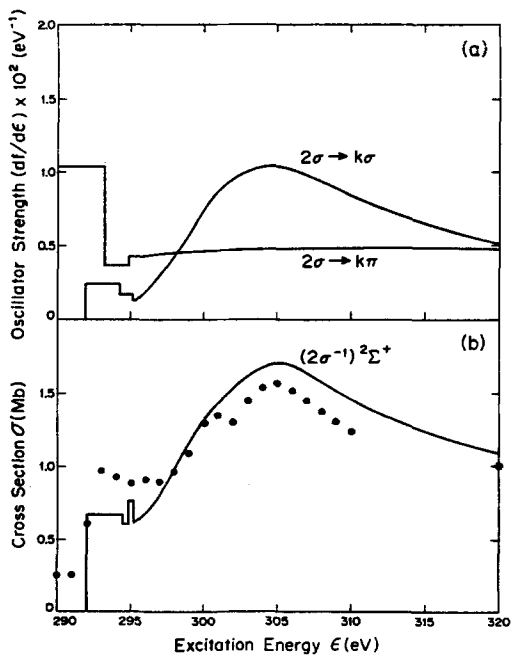

FIG. 6. As in Fig. 1(a) for $2\sigma \rightarrow k\sigma$ and $2\sigma \rightarrow k\pi$ photoionization. (b) Photoabsorption cross section near the C K edge in CO; (——), vertical electronic IVO S–T cross section (the $2\sigma \rightarrow 2p\pi$ resonance contribution is deleted); •, electron–ion coincidence measurements (Ref. 15). 1 Mb = 10^{-18} cm^2.

TABLE V. 1σ (O_K-shell) excitation spectra in CO.

Present results[a]	Experimental values[b]
Energy (eV)/f number	Energy (eV)/intensity
$(1\sigma)^1\Sigma^+ \rightarrow (ns\sigma)^1\Sigma^+$	
538.0/0.00191	538.8 $(3s\sigma)^1\Sigma^+$/weak
540.6/0.000266	...
541.4/0.00316	...
541.8/0.00097	...
542.0/0.00050	...
$(1\sigma)^1\Sigma^+ \rightarrow (np\sigma)^1\Sigma^+$	
540.1/0.00000	540.7 $(3p\sigma)^1\Sigma^+$/not observed[c]
541.2/0.00140	...
541.6/0.00550	...
541.9/0.00247	...
542.1/0.00161	...
$(1\sigma)^1\Sigma^+ \rightarrow (np\pi)^1\Pi$	
530.1/0.132	534.0 $(2p\pi)^1\Pi$/strong
539.7/0.00102	539.8/weak
541.1/0.00113	...
541.6/0.00073	...
541.9/0.00046	...

[a]As in Table I.
[b]As in Table IV.
[c]Position assigned on basis of an analogy with the observed CF valence spectrum (see Ref. 30).

In Fig. 7(a) are shown the convergent IVO S–T $1\sigma \rightarrow k\sigma$ and $k\pi$ photoionization cross sections in CO. These are remarkably similar to the corresponding $2\sigma \rightarrow k\sigma$ and $k\pi$ cross sections, but are approximately one-half the value of the latter and, of course, shifted to higher energy. Although quantitative values of the total oxygen K-edge cross section in CO are apparently not available at present, the shape of the measured relative photoionization spectrum is in agreement with the total IVO cross section shown in Fig. 7(b), and contains a resonancelike structure at ~ 550 eV excitation energy.[30] Of course, convolution of the measured qualitative spectrum with an appropriate instrument function can shift the peak somewhat, although the effect should not be a significant one. As in Fig. 6(b), the contribution of the strong resonance to the total 1σ photoabsorption cross section has been deleted for clarity in Fig. 7(b).

V. CONCLUDING REMARKS

Discrete-basis-set variational calculations and the Stieltjes–Tchebycheff technique are employed in investigations of vertical electronic photoexcitation and ionization cross sections in carbon monoxide. Static-exchange or improved-virtual-orbital eigenfunctions and eigenvalues are constructed for one-electron dipole excitations of the six occupied molecular orbitals, corresponding to configuration-interaction calculations in which a frozen core is maintained in each case. Some allowance is made for the effects of core relaxation by employing experimentally determined ionization potentials in the construction of transition energies, insuring that the theoretically determined Rydberg series converge to the appropriate limits. The pseudospectra of transition frequencies and oscillator strengths corresponding to continuum excitations are used in representing the appropriate photoionization cross section in a Stieltjes–Tchebycheff moment analysis. In this way IVO S–T approximations are obtained to the complete photoexcitation and ionization cross section in carbon monoxide, employing only familiar quantum-mechanical L^2 variational calculations of the type appropriate for bound-state investigations.

The calculated photoabsorption cross sections are compared with the available very detailed spectral-position and intensity data. Particularly good agreement between theory and experiment is obtained for the frequencies and strengths of the discrete valencelike and Rydberg transitions in carbon monoxide. Although autoionizing line shape calculations are not reported, the total integrated intensity in the valence-orbital $(5\sigma, 1\pi, 4\sigma)$ spectral excitation energy interval, measured by electron–ion coincidence techniques, is satisfactorily predicted. Similarly, the partial photoionization cross sections corresponding to ejection of electrons from 5σ, 1π, or 4σ orbitals are in good accord with recent branching-ratio and total intensity measurements. Predicted shape-resonance structures in both the $5\sigma \rightarrow k\sigma$ and $4\sigma \rightarrow k\sigma$ channels are in particularly good agreement with the corresponding measured profiles. These features are attributed to the presence of $k\sigma^*$ valencelike orbitals in the photoionization continuum,

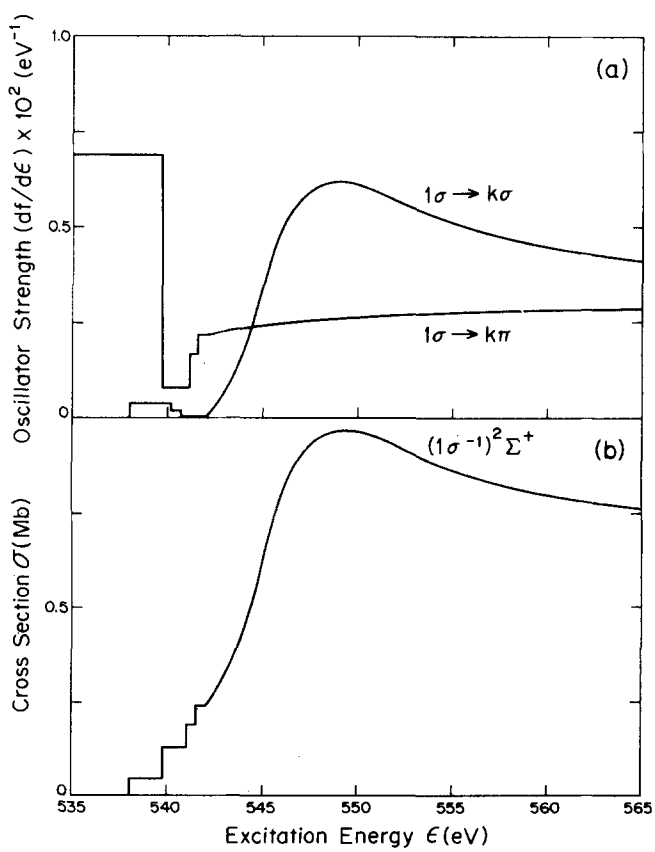

FIG. 7. (a) As in Fig. 1(a) for $1\sigma \rightarrow k\sigma$ and $1\sigma \rightarrow k\pi$ photoionization. (b) As in Fig. 6(b) for the O K edge in CO.

positioned there by the inability of the effective potential to support a bound σ^* orbital. Previously reported studies of photoionization in molecular nitrogen reveal the presence of a corresponding $3\sigma_g \rightarrow k\sigma_u$ shape resonance, although the inversion symmetry in this case prevents the appearance of a similar structure in the $2\sigma_u \rightarrow k\sigma_g$ channel. The theoretically determined 3σ channel cross section in carbon monoxide also contains a broad resonance feature, and is in general accord with corresponding measurements of the production of C^+–O and C–O^+ fragments. Finally, the carbon and oxygen K-edge cross-section calculations show strong $\sigma \rightarrow \pi^*$ transitions below the ionization limits and broad $\sigma \rightarrow \sigma^*$ resonance structures above, in good agreement with available measurements.

Although the very good agreement obtained between measured cross sections and separated-channel static-exchange calculations is satisfying, the use of only L^2 functions in the theoretical development is perhaps the most significant aspect of the present work. These results, and the results of related L^2 photoionization/absorption studies in other diatomic and polyatomic molecules, indicate that the very formidable technology of computational quantum chemistry can be used successfully in investigations of molecular electronic photoionization continua.

ACKNOWLEDGMENTS

The authors gratefully acknowledge the financial support of the US–Latin American Science Program, NSF(OIP)-CNPq (Brazil), of the FAPESP (São Paulo, Brazil), of the BID, and of the Donors of the Petroleum Research Fund, administered by the American Chemical Society. They also thank Professor Sergio Porto for his support of the cooperative project, Professor J. E. Ripper for making BID support available, Professor Nelson Machado for efficient operation of the Computing Center, Universidade Estadual de Campinas, where the calculations were performed, and Guillermo Barrera, Dante Ming Valent, and Marisa de Souza for computational assistance.

[1]R. S. Mulliken and C. A. Rieke, Rep. Prog. Phys. **8**, 231 (1941).
[2]G. Herzberg, *Spectra of Diatomic Molecules* (Van Nostrand, New York, 1950), 2nd edition.
[3]B. Schneider and R. S. Berry, Phys. Rev. **182**, 141 (1969).
[4]H. C. Tuckwell, J. Phys. B **3**, 293 (1970).
[5]J.-T. J. Huang, F. O. Ellison, and J. W. Rabalais, J. Electron Spectrosc. Relat. Phenom. **3**, 339 (1974).
[6]S. Iwata and S. Nagukura, Mol. Phys. **27**, 425 (1974).
[7]C. Duzy and R. S. Berry, J. Chem. Phys. **64**, 2421 (1976).
[8]F. Hirota, J. Electron Spectrosc. Relat. Phenom. **9**, 149 (1976).
[9]*Photoionization and Other Probes of Many-Electron Interactions*, edited by F. J. Wuilleumier (Plenum, New York, 1976).
[10]E. W. Plummer, T. Gustafsson, W. Gudat, and D. E. Eastman, Phys. Rev. A **15**, 2339 (1977).
[11]J. A. R. Samson and J. L. Gardner, J. Electron Spectrosc. Relat. Phenom. **8**, 35 (1976).
[12]J. A. R. Samson, G. N. Haddad, and J. L. Gardner, J. Phys. B **10**, 1749 (1977).
[13]A. Hamnett, W. Stoll, and C. E. Brion, J. Electron Spectrosc. Relat. Phenom. **8**, 367 (1976).
[14]G. R. Wight, M. J. Van der Wiel, and C. E. Brion, J. Phys. B **9**, 675 (1976).
[15]R. B. Kay, Ph. E. Van der Leeuw, and M. J. Van der Wiel, J. Phys. B **10**, 2513 (1977).
[16]L. C. Lee, R. W. Carlson, D. L. Judge, and M. Ogawa, J. Quant. Spectrosc. Radiat. Transfer **13**, 1023 (1973).
[17]P. Gürtler, V. Saile, and E. E. Koch, Chem. Phys. Lett. **48**, 245 (1977).
[18]C. M. Dutta, F. M. Chapman, and E. F. Hayes, J. Chem. Phys. **67**, 1904, 2974 (1977).
[19]P. W. Langhoff, S. R. Langhoff, and C. T. Corcoran, J. Chem. Phys. **67**, 1722 (1977).
[20]J. L. Dehmer and D. Dill, J. Chem. Phys. **65**, 5327 (1976).
[21]J. W. Davenport, Int. J. Quantum Chem. S **11**, 89 (1977).
[22]T. N. Rescigno and P. W. Langhoff, Chem. Phys. Lett. **51**, 65 (1977).
[23]T. N. Rescigno, C. F. Bender, B. V. McKoy, and P. W. Langhoff, J. Chem. Phys. **68**, 970 (1978).
[24]P. W. Langhoff, C. T. Corcoran, J. S. Sims, F. Weinhold, and R. M. Glover, Phys. Rev. A **14**, 1042 (1976).
[25]C. T. Corcoran and P. W. Langhoff, J. Math. Phys. **18**, 651 (1977).
[26]P. H. Krupenie, Natl. Stand. Ref. Data Ser. Natl. Bur. Stand. **5** (1966).
[27]E. Lindholm, Ark. Fys. **40**, 111 (1969).
[28]E. N. Lassettre and A. Skerbele, J. Chem. Phys. **54**, 1597 (1971).
[29]J. Mazeau, C. Schermann, and G. Joyez, J. Electron Spectrosc. Relat. Phenom. **7**, 269 (1975).
[30]G. R. Wight, C. E. Brion, and M. J. Van der Wiel, J. Electron Spectrosc. Relat. Phenom. **1**, 457 (1973).
[31]J. C. Tully, R. S. Berry, and B. J. Dalton, Phys. Rev. **176**, 95 (1968).
[32]U. Fano and J. W. Cooper, Rev. Mod. Phys. **40**, 441, (1968).
[33]H. A. Bethe and E. E. Salpeter, *Quantum Mechanics of One- and Two-Electron Atoms* (Springer, Berlin, 1957).
[34]G. Breit and H. A. Bethe, Phys. Rev. **93**, 888 (1954).
[35]A. Temkin, K. V. Vasavada, E. S. Chang, and A. Silver, Phys. Rev. **186**, 57 (1969).
[36]H. F. Schaefer III, *The Electronic Structure of Atoms and Molecules* (Addison-Wesley, Reading, MA 1972).
[37]J. B. Rose and B. V. McKoy, J. Chem. Phys. **55**, 5435 (1971).
[38]H. P. Kelly, Phys. Rev. **136**, 896 (1964).
[39]P. W. Langhoff, M. Karplus, and R. P. Hurst, J. Chem. Phys. **44**, 505 (1966).
[40]W. J. Hunt and W. A. Goddard, Chem. Phys. Lett. **3**, 414 (1969); **24**, 464 (1974).
[41]S. V. O'Neil and H. F. Schaefer III, J. Chem. Phys. **53**, 3994 (1970).
[42]H. Lefebvre-Brion, C. M. Moser, and R. K. Nesbet, J. Mol. Spectrosc. **13**, 418 (1964).
[43]P. W. Langhoff and S. W. Chan, Mol. Phys. **25**, 345 (1973).
[44]R. Marriott and M. J. Seaton, Proc. Phys. Soc. London Sect. A **70**, 296 (1957).
[45]T. N. Rescigno, J. Chem. Phys. **66**, 5255 (1977).
[46]K. Siegbahn, C. Nordling, G. Johansson, J. Hedman, P. F. Hedén, K. Hamrin, V. Gelius, T. Bergmark, L. O. Werme, R. Manne, and Y. Baer, *ESCA Applied to Free Molecules* (North-Holland, Amsterdam, 1969).
[47]W. J. Rabalais, *Principles of Ultraviolet Photoelectron Spectroscopy* (Wiley, New York, 1977).
[48]S. R. Smith and T. Darrah-Thomas, J. Electron Spectrosc. Relat. Phenom. **8**, 45 (1976).
[49]P. W. Langhoff, J. Chem. Phys. **57**, 2604 (1972).
[50]C. T. Corcoran and P. W. Langhoff, Chem. Phys. Lett. **41**, 609 (1975); P. M. Johnson, P. W. Langhoff, S. V. O'Neil, C. T. Corcoran, and W. P. Reinhardt, Chem. Phys. Lett. **52**, 380 (1977).
[51]J. A. Shohat and J. D. Tamarkin, *The Problem of Moments*,

Mathematical Surveys 1 (American Mathematical Society, Providence, RI, 1943).
[52]T. H. Dunning, J. Chem. Phys. **53**, 2823 (1970).
[53]R. S. Mulliken, Acc. Chem. Res. **9**, 7 (1976).
[54]A. U. Hazi, J. Phys. B **11**, L259 (1978).
[55]A. W. Weiss, Phys. Rev. **178**, 82 (1969).
[56]C. F. Bender, V. McKoy, and E. Davidson, J. Chem. Phys. **67**, 2178 (1977).
[57]The valence-state calculations of S. V. O'Neil and H. F. Schaefer (Ref. 41) predict a dissociative $(\pi \rightarrow \pi^*)\,^1\Sigma^+$ state having a vertical excitation energy of ~ 15.5 eV, as well as a $(\sigma \rightarrow \sigma^*)\,^1\Sigma^+$ state in the photoionization continuum. When interaction with the underlying Rydberg states is introduced, the the appearance of local minima in the adiabatic potential curves can be anticipated, although the intensity of the $\pi \rightarrow \pi^*$ transition will follow the diabatic curve. See for example, W. Coughran, J. Rose, T. Shibuya, and V. McKoy, J. Chem. Phys. **58**, 2699 (1973). S. R. Langhoff (private communication) has recently completed CI studies of Rydberg–$(\pi \rightarrow \pi^*)$ state interactions in CO which generally support these observations.
[58]M. Okuda and N. Jonathan, J. Electron Spectrosc. Relat. Phenom. **3**, 19 (1974).
[59]P. S. Bagus and E. Viinikka (unpublished).
[60]M. Nakamura, M. Sasanuma, S. Sato, M. Watanabe, H. Yamashita, Y. Iguchi, A. Ejiri, S. Nakai, S. Yamaguchi, T. Sagawa, Y. Nakai, and T. Oshio, Phys. Rev. **178**, 80 (1969).
[61]A similar situation is encountered in the previously reported IVO calculations of the K-edge photoabsorption cross section in N_2 (Ref. 22). In this case relaxation effects are perhaps most conveniently introduced by employing broken symmetry orbitals. See, for example, G. C. King, F. H. Read, and M. Tronc, Chem. Phys. Lett. **52**, 50 (1977); W. Domcke and L. S. Cederbaum, Chem. Phys. **25**, 189 (1977); R. A. Martin and E. R. Davidson, Phys. Rev. A **16**, 1341 (1977).
[62]M. J. Van der Wiel, Th. M. El-Sherbini, and C. E. Brion, Chem. Phys. Lett. **7**, 161 (1970).